Ceramics-Silikáty 65 (2), 176-186 (2021)
www.ceramics-silikaty.cz doi: 10.13168/cs.2021.0017

EFFECT OF MUNICIPAL SLUDGE ON THE PERFORMANCE OF COAL GASIFICATION SLAG-BASED CERAMSITE

LI KUNJIE*, WANG JUN**, #MA JIANFENG**, GAO DA**, BI YAO**, LUO YAOLING**, CHEN XIAORUN**

*Stuart School of Business of Illinois Institute of Technology, Chicago, 60608, USA
**China West Construction Academy of Building Materials, Chengdu, 610000, China

#E-mail: 991461390@qq.com

Submitted October 30, 2020; accepted April 10, 2021

Keywords: Municipal sludge, Coal gasification slag-based ceramsite, Pore structure, Oxide content

Ceramsite was sintered using coal gasification slag, fly ash, construction spoils, and municipal sludge. The influence of the municipal sludge content on the ceramsite performance was studied by TG-DSC, XRD, MIP, and SEM. The optimal sintering conditions for the fabrication of ceramsite exhibiting the best performance were obtained through an orthogonal experiment. The highest cylindrical compressive strength was obtained under the following conditions: a preheating temperature of 500 °C with a preheating time of 30 min, and a sintering temperature of 1100 °C with a sintering time of 20 min. The compressive strength of the ceramsite was higher than 6.5 MPa when the municipal sludge content was 20 % and prepared in optimal conditions. The porosity and the average pore diameter of the ceramsite increased with an increasing municipal sludge content, while the strength and apparent density decreased. The average pore diameter of the ceramsite with the 20 % municipal sludge content increased by 490 nm compared with the ceramsite containing a 5 % municipal sludge. In addition, the Al_2O_3 content was the factor affecting the strength of the ceramsite. When the Al_2O_3 content exceeded 20.5 %, the main crystal phase of the ceramsite changed from a quartz phase to kyanite, significantly improving its strength.

INTRODUCTION

Municipal sewage sludge is a type of fluid waste formed after treatment in a municipal sewage treatment plant, and its water content is typically 80 %. It is generally black or dark brown, and its organic content is higher than 40 %. Municipal sludge contains a large number of pathogens, parasite eggs, heavy metals, and many harmful pollutants [1, 2]. With a continuous increase in industrialisation and urbanisation, the annual output of municipal sludge continues to increase. For example, China produced approximately 1.5 million tonnes of municipal sludge in 2018. Therefore, a reasonable and effective treatment of municipal sludge has become a very important topic. In particular, resource treatment has become one of the most effective ways to treat municipal sludge [3-5].

The use of municipal sludge to make ceramsite, ceramic tiles, and insulation bricks is one of the main technologies for the disposal of municipal sludge [6-8]. In recent years, the main concern regarding municipal sludge ceramsite has been the sintering and swelling process of municipal sludge ceramists. For example, Xu [9] et al. proposed that ceramsite with an excellent performance could be obtained at sintering temperatures above 1000 °C. Ding et al. [10] showed that the preheating temperature was the main factor affecting the swelling of ceramsites. Specifically, optimal expansion properties of sludge ceramsites were obtained when the preheating temperature was approximately 400 °C. Liu [11] et al. demonstrated that the production of gas is the main reason for the formation of pores in ceramsite.

The strength of ceramsite containing municipal sludge is generally low, and it has been generally used in non-load-bearing insulation materials. For example, Qin [12] et al. used municipal sludge, fly ash, and diatomaceous earth to sinter ceramsite with a compressive strength of 4.73 MPa, and the water absorption rate was as high as 39.03 %. Liu et al. [13] developed ceramsite sintered from municipal sludge, calcium carbonate, and sea mud with a compressive strength of 5.35 MPa and a water absorption rate of 13.34 %. Su et al. [14] used municipal sludge, fly ash, and bentonite to sinter ceramsite with a compressive strength of 3.05 MPa.

In addition, researchers have studied the effect of municipal sludge on the performance of ceramsite while adding oxides to the mixture. Qin et al [15] showed that a proper SiO_2 content was beneficial to the performance of ceramsite, but a too high or too low SiO_2 content was detrimental to its strength. Zuo et al. [16] studied the content of Fe_2O_3, CaO, and MgO on the performance of ceramsite. The results showed that the porosity of

ceramsite decreased while the strength increased with an increasing Fe_2O_3. In addition, a high CaO and MgO content were detrimental to the strength of the material. Xu et al. [17] proved that the $(Fe_2O_3+CaO+MgO)/(SiO_2+Al_2O_3)$ ratio greatly determines the properties of ceramsite. For example, a ceramsite with a higher compressive strength and lower porosity was obtained with a $(Fe_2O_3+CaO+MgO)/(SiO_2+Al_2O_3)$ ratio from 0.175 to 0.275.

Based on the above research, the influence of the sintering system of municipal sludge-based ceramsite, swelling ceramsite, and the oxide content on its performance is relatively mature. Moreover, a better-performing ceramsite containing municipal sludge can be realised using a supplementary oxide in the mixture. However, this may increase the cost of the ceramsite and limit its application in practical engineering.

At present, most of the ceramsites with the best properties were prepared from solid waste containing shale, fly ash, clay, and glass powder, among others [18-20]. However, as the main mineral admixture in concrete, the cost of fly ash has increased in recent years. In addition, ceramsite sintered with fly ash as the main material had a high water absorption rate (generally above 10 %), which harmed the performance of the lightweight aggregate concrete. Additionally, the performance of ceramsite sintered from other types of solid waste was poor [13, 14, 21].

Coal gasification slag is a solid waste produced during the process of coal gasification. According to the statistics, China's coal gasification slag output exceeded 33.5 million tonnes in 2018 [22]. Coal gasification slag has been disposed of mainly in landfills, and large-scale industrial applications have not yet been made widely available [23]. Studies determined that coal gasification slag is mainly composed of SiO_2, Al_2O_3, CaO, Fe_2O_3, and C, among others, and its main mineral phase is amorphous silicate, quartz, and calcite [24]. Therefore, coal gasification slag fully meets the requirements of the raw materials for production of ceramsite [25]. However, there are not many studies on ceramsite sintered with coal gasification slag as the main raw material.

Therefore, in this paper, coal gasification slag was used as the main raw material to sinter ceramsite, and mixtures with a municipal sludge dosage (0-20 %) on the performance of ceramsite was analysed. The physic-mechanical properties of the ceramsite, including the water absorption rate, particle density, and compressive strength, were studied. The pore structure and phase change of the ceramsite were analysed through Scanning Electron Microscopy (SEM), mercury intrusion porosimetry (MIP) and X-ray powder diffraction (XRD). On this basis, combined with the physical characteristics, the ceramsite was analysed to determine the effect of the municipal sludge content on the properties of the ceramsite.

EXPERIMENTAL

Materials and ceramsite preparation process

Materials

The municipal sludge used in this study was obtained from a sewage treatment plant in Chengdu, Sichuan Province, China, and the water content was approximately 80 %. The sludge was dried at 105 °C and ground before being used due to its high water content. The construction spoils were obtained from the spoils of a construction site in Chengdu, Sichuan Province, China, the fly ash was acquired from a power plant in Chengdu, Sichuan Province, China, and the coal gasification slag was obtained from the waste product after the coal gasification process in Taiyuan, Shanxi Province, China. The samples were analysed by X-ray fluorescence spectroscopy (Shimadzu XRF-1700), and the results are shown in Table 1. The oxides present in

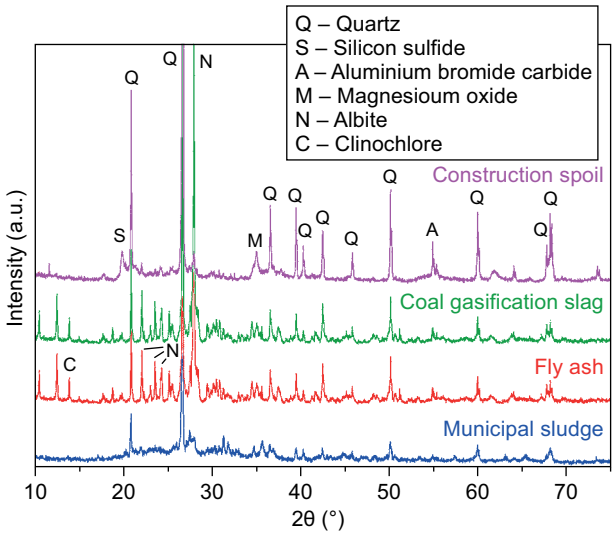

Figure 1. XRD spectrum of the raw materials.

Table 1. Chemical composition of the materials.

Raw materials	SiO_2	Al_2O_3	Fe_2O_3	Na_2O	MgO	CaO	K_2O
Municipal sludge	30.95	18.79	8.15	0.83	4.71	8.05	4.22
Fly ash	50.39	27.49	8.47	1.41	0.95	1.47	2.03
Coal gasification slag	45.44	26.37	9.29	0.91	1.11	12.30	1.28
Construction spoils	70.03	17.15	5.49	0.97	1.41	0.79	2.72

each raw material are mainly SiO_2 and Al_2O_3. Figure 1 shows the XRD patterns. The crystalline phases of the test materials were analysed by XRD (D/MAX-IIIC X-ray diffract meter). As shown in Figure 1, the major minerals of the raw materials were quartz and its oxides, as well as aluminium-containing oxides. Figure 2 shows the Thermogravimetry-Differential Scanning Calorimetry (TG-DSC) curve of the raw materials. The results show that the weight loss of the municipal sludge was significant, while the loss of the other raw materials was not.

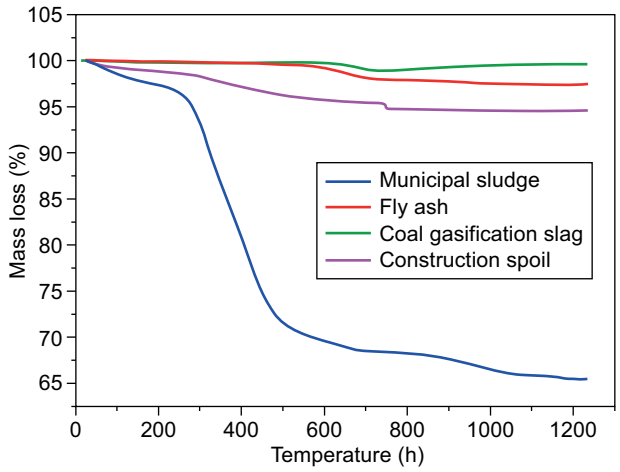

a) TG

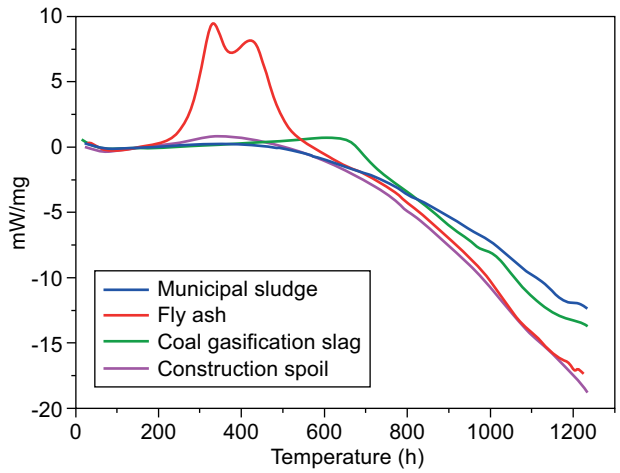

b) DSC

Figure 2. TG-DSC of raw materials.

Ceramsite preparation process

Figure 3 presents the preparation process of the ceramsite used in this study, which is similar to that described by Yong et al. [26]. The municipal sludge, fly ash, construction spoils, and coal gasification slag were crushed and then sieved through a number 200 mesh sieve. The particle size analysis was carried out using a laser granularity analyser (Microtrac S3500 laser particle size analyser, Microtrac Inc.) and Figure 4 presents the particle size distribution of the sieved materials. The materials were then dried and mixed at the required proportion, and then poured into meal ball granules, 5 - 25 mm in diameter. The meal ball granules were transferred into a box resistor furnace and then preheated at 400 - 600 °C. Later, they were sintered at a sintering temperature of 1000 - 1200 °C for 10 - 50 min. After sintering, the ceramsites were cooled to room temperature by natural convection.

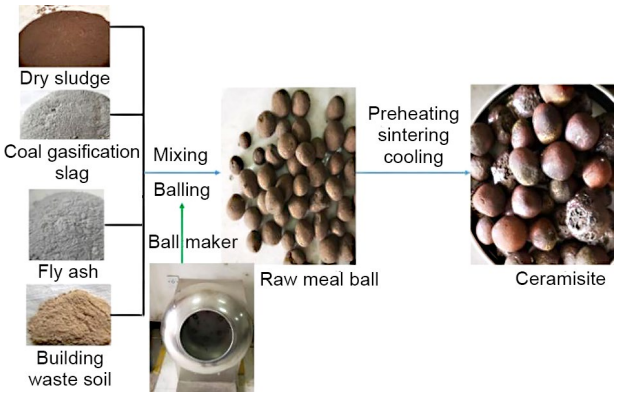

Figure 3. Fabrication process of the ceramsite.

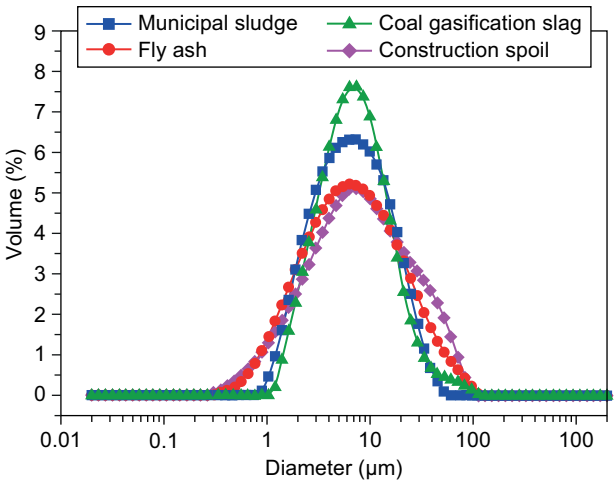

Figure 4. Particle size distribution of the raw materials.

Table 2 shows the compositions of the different samples with their corresponding municipal sludge, SiO_2, and Al_2O_3 content.

Table 2. Municipal sludge and the oxide content of the mixtures (%).

Samples	Municipal sludge	SiO_2	Al_2O_3	Fe_2O_3	MgO	CaO
A1	5	56.29	23.83	7.41	3.13	3.36
A2	5	62.94	19.43	6.21	2.10	1.89
B1	10	53.59	21.78	6.81	2.61	2.63
B2	10	60.23	20.41	6.65	2.51	2.62
C1	20	52.38	22.64	7.51	3.36	2.67
C2	20	58.32	17.64	7.27	1.62	6.12

Analysis

The 1 h water absorption rate, compressive strength, and apparent density of the ceramsite samples were determined according to methods specified in the Chinese standard "Lightweight Aggregate and Its Test Method" (GBT17431.1-2010) [27]. According to the standard, the 1 h water absorption test method of the ceramsite consisted of weighing a certain quantity of ceramsite (m_1) and soaking it in water for 1 h. Then, the ceramsite was removed from the water, the surface water on the ceramsite was removed with a wet towel, and the new weight was recorded as m_n. The 1 h water absorption rate of the ceramsite was then calculated according to Equation 1.

$$\omega_n = \frac{m_n - m_1}{m_1} \times 100\ \% \tag{1}$$

where ω_n is the water absorption rate of the ceramsite soaked in water for n hours, m_n is the mass after the ceramsite has absorbed water for n hours, and m_1 is the mass of the dry ceramsite.

The compressive strength of the ceramsite was tested according to the National Standard of the People's Republic of China (GB/T 17431.2-2010) [28]. The compressive strength of the ceramsite was measured using a cylindrical pressure-bearing mould as shown in Figure 4. The procedure consisted of filling the mould with ceramsite and manually making it vibrate for 5 - 10 s by means of one's hands. This procedure was repeated until the mould was completely filled with material. Then, the pressure-bearing cylinder was placed on the lower pressure plate of the press and aligned to the centre. The load was set at a constant speed of 300 ~ 500 N per second. When the pressing depth of the stamping die was 20 mm, the pressure was recorded. The final compressive strength value of the ceramsite was determined according to Equation 2. Each group of samples was tested 3 times and the average value was calculated.

$$f_n = \frac{p_1 + p_2}{F} \tag{2}$$

where f_n is the compressive strength of the ceramsite cylinder (MPa), p_1 is the pressure value (N) when the indentation depth is 20 mm, p_2 is the quality of the punched film (N), and F is the pressure-bearing area.

The measurement of the apparent density consisted of first weighing a certain quantity of dry ceramsite, recorded as m. The ceramsite was then introduced into water for 1 h, the surface was dried with a wet towel, and the sample was placed into a measuring cylinder. Then, 500 ml of water was poured into the graduated cylinder and the volume V was recorded. Finally, Equation 3 was used to calculate the apparent density of the ceramsite.

$$\rho = \frac{m \times 1000}{v - 500} \tag{3}$$

where ρ is the apparent density of the ceramsite (kg·m^{-3}), m is the mass of the ceramsite under dry conditions, and V is the total volume of the ceramsite after water absorption and the addition of 500 ml of water (ml).

The physicochemical changes that the raw materials underwent during the sintering of the ceramsite were analysed using thermo gravimetric-differential thermal scanning calorimetry (TGA-DSC) (NETISCH, Germany, STA409C). After mixing uniformly, the raw materials were ground with a grinding body and passed through a square hole sieve of 80 microns or larger. The samples were placed into the equipment and heated at a rate of 8 °C·min^{-1} from 20 to 1080 °C in air. Between 4 and 10 mg of the sample were weighed, and they were put into a Pt-Rh crucible with 20 taps. All the curves were evaluated using the TA-instruments software.

To evaluate the microstructure of the ceramsite samples, the sintered ceramsite was cut into 3 - 5 mm slices and then adhered to a conductive adhesive. After gold spraying, images were taken using an SEM/EDS by a Tescan VEGA III LMU scanning electron

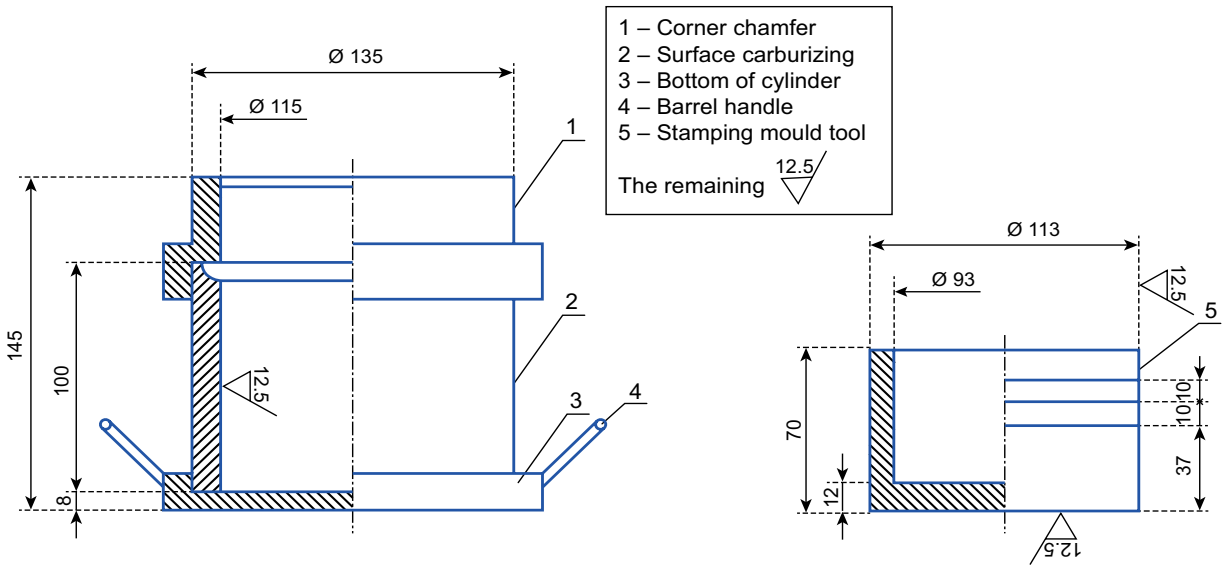

Figure 5. Mould pattern for the analysis of the compressive strength of the ceramsite.

microscope (SEM). The high vacuum resolution used was 3.0 nm/30 kV, and the low vacuum resolution was 3.5 nm/30 kV. The magnification was 4 ~ 100 000 times, the operating voltage was 0.2 ~ 30 kV, and the electron beam current was 1 ~ 2 pa

The pore structure of the ceramsite was determined using mercury intrusion porosimetry (MIP). The sintered ceramsite was crushed into particles approximately 3 - 5 mm in diameter and 2 - 3 g of each specimen was used. The mercury intrusion was performed on an AutoPore® IV 9510 equipment (Micromeritics Instrument Corp). The ceramsite was placed in the equipment and then the pressure was increased from atmospheric pressure to a maximum pressure of p_{max} = 414 MPa, and then released to atmospheric pressure again. The raw data was analysed using the Washburn equation.

To analyse the phases and chemical composition of the ceramsite, the material was first ground into a powder, and a D/MAX-IIIC X-ray diffractometer was used to analyse the sample. The target material of the instrument was copper, the scanning range was 5 - 70°, and the scanning speed was 2.5° per minute.

RESULTS AND DISCUSSION

Sintering of ceramsite

The rates of the weight loss of the mixtures were examined at different temperatures and the results are shown in Figure 6. Figure 6a presents the mass loss during the heating process, and Figure 6b is the endothermic/exothermic change in the process.

It can be seen from Figure 6a that the weight loss of the mixtures increased with an increasing municipal sludge content. Specifically, the weight loss of the mixtures with a 20 % municipal sludge content was approximately 12 % greater than that of samples with a 5 % municipal sludge content. This suggests that a significant weight loss of the mixtures is due to the municipal sludge. For the mixtures with a municipal sludge content of 20 %, the weight loss of sample C1 was greater than that of sample C2 during the heating process, which was caused by the different raw materials and their content.

Furthermore, it can be seen from Figure 6a that the weight loss of the mixtures occurred in the range of 300 ~ 500 °C. When the temperature was higher than 700 °C, the weight of the material remained unchanged. As observed in Figure 6b, three endothermic peaks appeared during the heating process. The first exothermic peak can be observed at approximately 320 °C, and a secondary exothermic peak at 450 °C. These two peaks were due to the decomposition of the organic compounds contained in the mixtures [29]. The third exothermic peak at temperatures higher than 600 °C suggests the polymorphic transformation of the quartz [30].

In order to obtain the optimal ceramsite sintering conditions, mixture B1 with a municipal sludge content of 10 % was selected for the sintering test. The thermal effect of the mixtures during the high-temperature thermal processing have been previously investigated using TG-DSC measurements. Therefore, the preheating temperature was selected as 400, 450 and 500 °C for 10 min, 20 min, and 30 min, respectively. The sintering temperature was varied between 1050, 1100 and 1150 °C, and the corresponding sintering time was 10, 20 and 30 min. Table 3 shows the orthogonal factor of mixture B1 and Table 4 shows the orthogonal test scheme of the sintering system of the B1 mixture with the 10 % of sludge content, and the compressive strength of the sintered ceramsite.

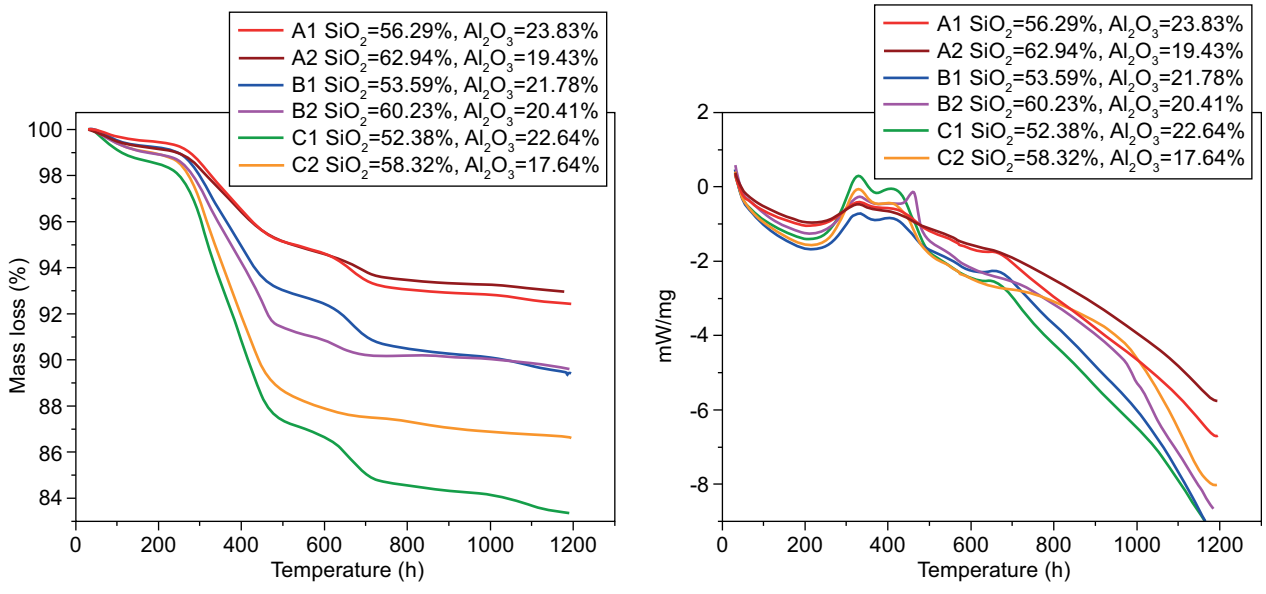

a) TG b) DSC

Figure 6. TG-DSC analysis of the mixtures.

Table 3. Orthogonal test factor level of the B1 mixture.

Level	Factor			
	A Preheating temperature (℃)	B Preheating time (min)	C Sintering temperature (℃)	D Sintering time (min)
1	400	10	1050	10
2	450	20	1100	20
3	500	30	1150	30

Table 4. Orthogonal test factor level of the B1 mixture.

	Factor level				Compressive strength (MPa)
	A Preheating temperature (℃)	B Preheating time (min)	C Sintering temperature (℃)	D Sintering time (min)	
D_1	1	1	1	1	4.2
D_2	1	2	2	2	4.9
D_3	1	3	3	3	4.9
D_4	2	1	2	3	4.8
D_5	2	2	3	1	4.6
D_6	2	3	1	2	4.8
D_7	3	1	3	2	5.1
D_8	3	2	1	3	4.9
D_9	3	3	2	1	5.2
k_1	4.67	4.70	4.63	4.67	–
k_2	4.73	4.77	4.93	4.90	–
k_3	5.07	4.97	4.87	4.87	–
R	0.40	0.27	0.30	0.23	–
σ	0.18	0.12	0.71	0.60	–
Optimal combination	$A_3B_3C_2D_2$				

It can be seen from Table 4 that the preheating and sintering temperatures were the main factors affecting the ceramsite strength, followed by the preheating and sintering time. When the preheating temperature was low and the preheating time was short, the organic matter in the ceramsite formed a gas and was discharged during the sintering process, causing the ceramsite to crack and the strength to be reduced. When the sintering temperature increased, the ceramsite melted and the pore content increased, which decreased the strength of the material. Therefore, the optimal conditions for the strength development were with a preheating temperature of 500 ℃, a preheating time of 30 min, a sintering temperature of 1100 ℃, and a sintering time of 20 min.

Performance of the ceramsite

Figure 7 shows the properties of the ceramsite fabricated under the optimal sintering conditions for the mixtures with the different municipal sludge content. As shown in Figure 7a, samples A1 and A2 with a municipal sludge dosage of 5 % had an apparent density of approximately 1800 kg·m^{-3}, and the water absorption rate for 1 h was the same at approximately 3.7 %. The apparent density of the ceramsite and the 1 h water absorption rate gradually decreased with an increasing municipal sludge content (group A to group C). Compared with the ceramsite of group A1 with 5 % municipal sludge, the 1 h water absorption rate of the ceramsite of group C1 with a 20 % sludge content increased by 5.3 %, and the apparent density decreased by 418 kg·m^{-3}.

In addition, it can be seen from Figure 7b that the strength of the ceramsite decreased with an increasing municipal sludge content. Compared with sample A1, the compressive strength of sample C1 with a 20 % of municipal sludge content was reduced by 3.3 MPa and the compressive strength of sample B1 with a 10 % of municipal sludge content was reduced by 2.8 MPa. However, sample A1 with the 5 % of municipal sludge content, sample B1 with a 10 % content, and sample C1 with a 20 % content all meet the requirements for a lightweight high-strength ceramsite according to GB/T 17431.1-2010 "Lightweight Aggregates and Test Methods"[28] (compressive strength > 6.5 MPa, density grade < 900 kg·m^{-3}).

In addition, the compressive strength was different for the ceramsite samples with the same amount of municipal sludge. For example, the comprehensive strength of sample A1 with a 5 % of sludge content was 4.2 MPa higher than that of sample A2. This may be caused by

the different SiO_2 and Al_2O_3 content in samples A1 and A2. On the other hand, the samples of group B with a sludge content of 10 % and group C with a content of 20 % showed the same change as group A. Therefore, for the ceramsite with the same municipal sludge content, it is necessary to study whether the change in strength was due to the change in the SiO_2 or Al_2O_3 content.

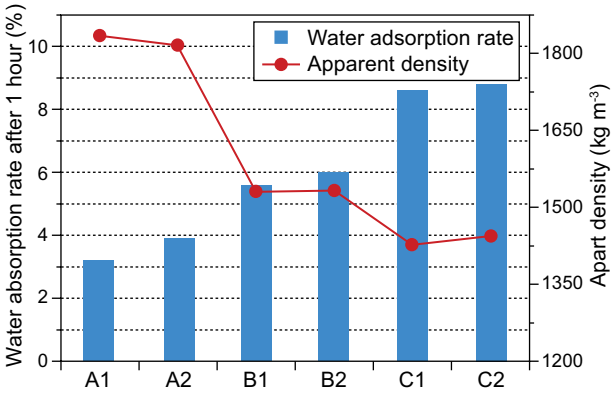

a) 1 h water absorption rate and apparent density

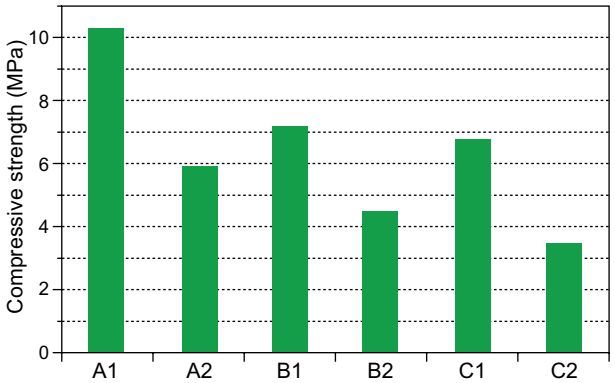

b) Compressive strength

Figure 7. The properties of the ceramsite.

Pore structure

The changes in the pore structure of the samples were analysed by the MIP mercury intrusion method. Figures 8 and 9 show the cumulative mercury intrusion and pore size distribution of each ceramsite sample, and the calculated pore size distribution and porosity values are shown in Table 5. The porosity and the average pore diameter of the ceramsite increased with an increasing municipal sludge content. For example, the cumulative mercury intrusion of sample A1 with a 5 % municipal sludge content was 0.031 $ml \cdot g^{-1}$ higher than that of ceramsite C2 with a 20 % municipal sludge content, and

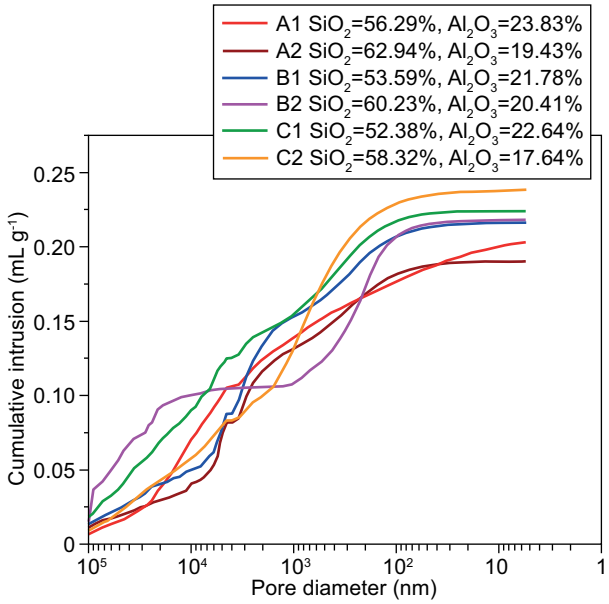

Figure 8. Cumulative mercury intrusion.

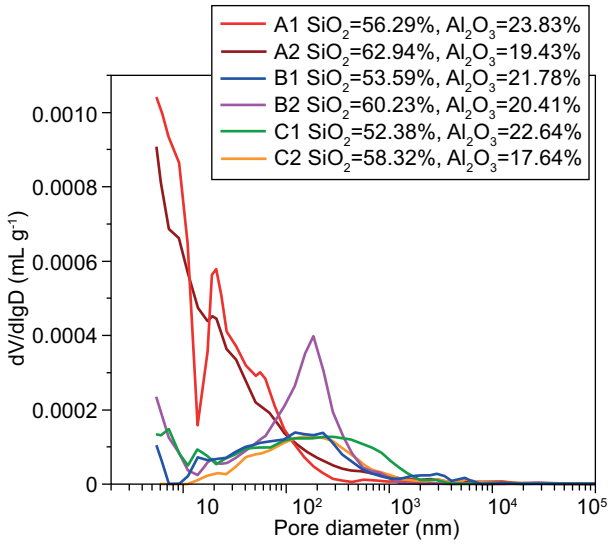

Figure 9. Differential curve of the pore size distribution of ceramsite samples.

Table 5. Porosity and pore size distribution of the ceramsite samples.

Samples	Cumulative mercury intrusion ($ml \cdot g^{-1}$)	Porosity (%)	Average pore size (nm)	Pore size distribution (%)		
				< 300 nm	300 ~ 10 000 nm	> 10 000 nm
A1	0.203	31.48	140.60	16.21	78.58	5.21
A2	0.206	32.05	147.27	20.95	65.46	13.59
B1	0.219	34.05	308.45	31.57	54.06	14.37
B2	0.216	34.38	413.01	16.81	66.90	16.29
C1	0.224	35.47	629.49	15.08	59.77	25.15
C2	0.229	35.21	480.34	14.64	65.78	19.58

the porosity was reduced by 3.99 %. The influence of the municipal sludge content on the porosity of the ceramsite could explain the changes in the water absorption and apparent density. More specifically, the increase in the porosity is beneficial for the water to enter into the material, and the apparent density of the ceramsite is reduced.

The pore size distributions of the ceramsite are shown in Figure 9. Each peak was the most probable pore diameter, which represents the highest probability of the occurrence in the ceramsite. As shown in Figure 9, the most probable pore diameter of the ceramsite samples with the same amount of municipal sludge was consistent for all the samples. For example, samples A1 and A2 with a 5 % municipal sludge content had the most probable pore diameter of approximately 20 nm, and those of group B with a 10 % municipal sludge content was approximately 200 nm. In addition, it can be seen from Table 5 that the pore diameter gradually increased with an increasing municipal sludge content. It is proposed that the municipal sludge could change the pore structure of the ceramsite due to the higher mass loss compared to other raw materials in the burning process.

In order to further study the influence of the municipal sludge on the pore structure of the ceramsite, SEM was used to observe the changes in the internal pore structure, as shown in Figure 10. It can be seen that the internal structure of the samples from group A with a 5 % municipal sludge content was compact, and the pore diameter was small when compared with samples from groups B and C. The internal pores of the group B ceramsite with a 10 % municipal sludge content were loose and the diameter was large. When the municipal sludge content reached 20 % (group C), the internal structure of the ceramsite was looser, and the

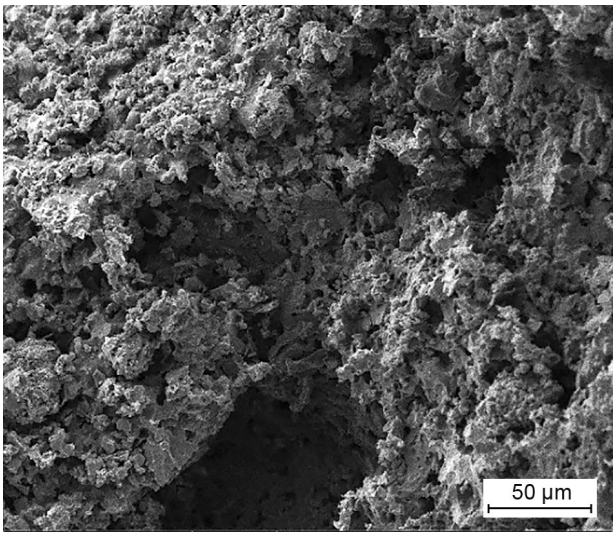

a) A1: SiO_2 = 56.29 %, Al_2O_3 = 23.83 %

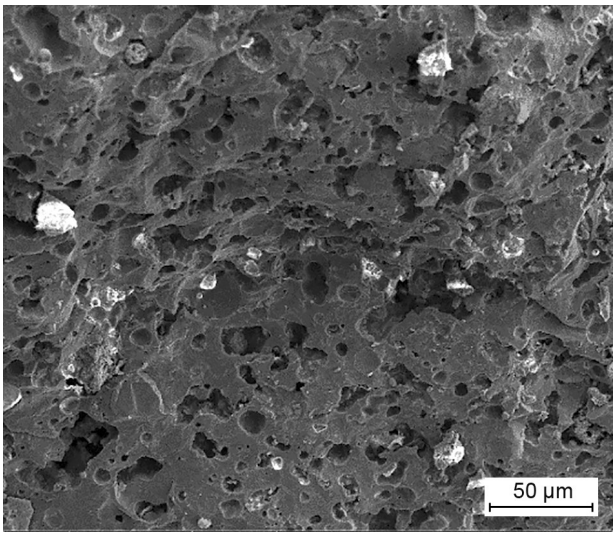

b) A2: SiO_2 = 62.94 %, Al_2O_3 = 19.43 %

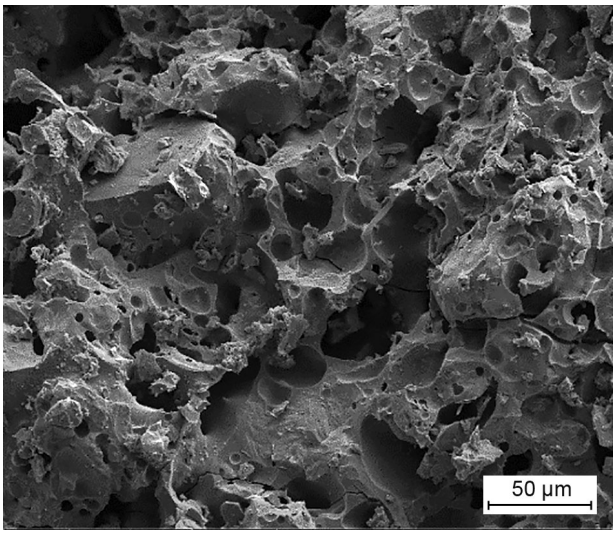

c) B1: SiO_2 = 53.59 %, Al_2O_3 = 21.78 %

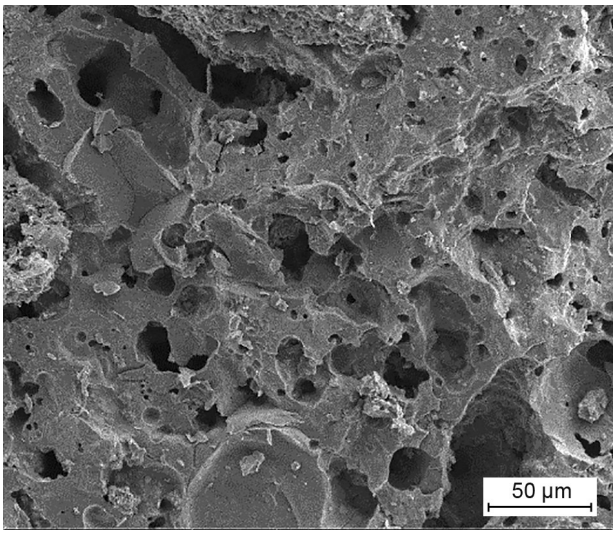

d) B2: SiO_2 = 60.23 %, Al_2O_3 = 20.41 %

Figure 10. Microscopic scan of the ceramsite samples. *(Continue on next page)*

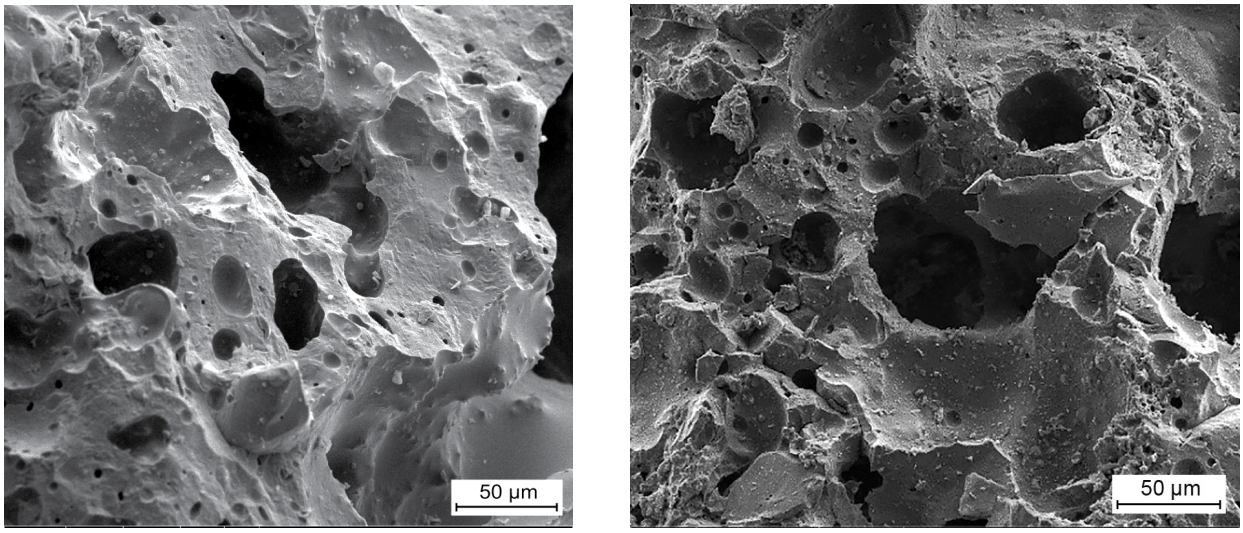

e) C1: SiO_2 = 52.38 %, Al_2O_3 = 22.64 %

f) C2: SiO_2 = 58.32 %, Al_2O_3 = 17.64 %

Figure 10. Microscopic scan of the ceramsite samples.

macropores increased significantly (> 10 000 nm pore size distribution), which was consistent with the MIP test results. Therefore, the increase in the amount of municipal sludge could reduce the strength of the ceramsite. The main reason is that as the content of the municipal sludge increases, the porosity and the average pore diameter increases, resulting in a loose internal structure, which is detrimental to its strength. This analysis is consistent with the conclusions in the literature [31-33].

XRD analysis

Figure 11 shows the XRD phase of the ceramsite, and Table 6 shows the change in the mineral content. It can be seen from Figure 10 that the main phases of ceramsite are quartz (SiO_2), kyanite (Al_2SiO_5), and a small amount of anorthite [albite-Na($AlSi_3O_8$), anorthite-Ca($Al_2Si_2O_8$)] and silicon limestone (Al_2SiO_5).

Table 6 shows that the main phase of ceramsite in group A1 was kyanite, while that of group A2 was quartz. The content of the municipal sludge in the Group A ceramsite was the same, therefore, this was not the reason for the phase change. It is worth noting that the SiO_2 content of ceramsite in group A1 decreased by 6.65 % and the content of Al_2O_3 increased by 4.4 % compared with that of group A2. In all the sample groups, the main crystal phase of the samples change from the quartz phase to kyanite as the content of Al_2O_3 increases. This shows that the change of the Al_2O_3content was the main reason for the phase change in the samples.

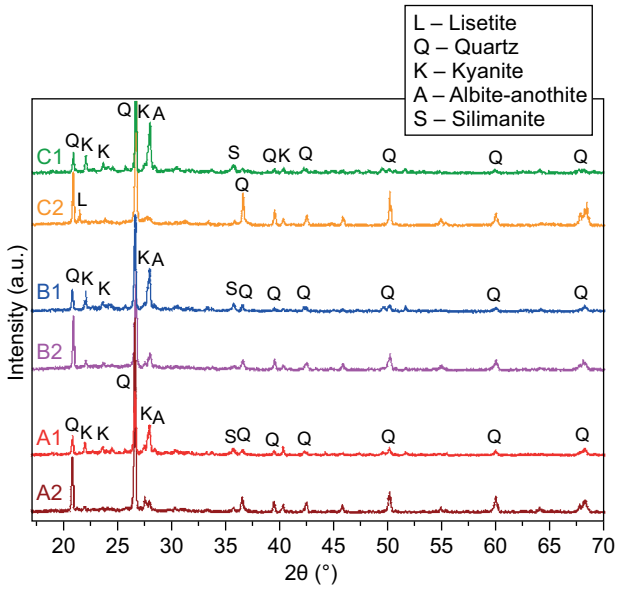

Figure 11. XRD patterns of the ceramsite samples.

Table 6. Crystal phases and corresponding phase content (%) in the ceramsite samples.

Samples	Quartz	Kyanite	Albite-anorthite	Sillimanite	Goethite
A1	19.0	64.0	15.7	1.3	–
A2	78.4	19.0	1.7	0.9	–
B1	27.8	55.5	14.4	2.3	–
B2	65.4	24.2	10.1	0.3	–
C1	29.9	47.7	21.7	0.7	–
C2	78.3	12.2	6.3	–	3.2

The main reason behind the phase change was that the Si in the silicon-oxygen framework had low coordination, so the [SiO_4] connected by the common top tends to be disconnected from each other. During the sintering process, the Al^{3+} ion is substituted for the Si^{4+} one in the network tetrahedron, contributing to the stability of the network, and Al_2O_3 could enter the silica network as an AlO_4^{4-} tetrahedra to replace some of the SiO_4^{4-} groups. In addition, the Al_2O_3 which had not replaced Si^{4+} was used as an oxide promoter to promote the pozzolanic reaction with the easily available alkali metal cations. This was beneficial to the strength of the ceramsite [16, 17, 34]. Therefore, at a constant sludge content, the strength of the ceramsite increased with an increasing Al_2O_3 content.

From the above results, it was determined that increasing the municipal sludge content increased the porosity of the ceramsite samples and the internal structure became loose, which, in turn, affected their strength. However, the amount of municipal sludge was not the only reason that affected the strength. A change in oxide content in ceramsite also affects the strength of the ceramsite. When the content of Al_2O_3 exceeded 20 %, the main crystal phase changed from quartz to kyanite, and the strength increased significantly. Therefore, it is necessary to comprehensively consider the impact of the municipal sludge and the oxide content on the performance of the ceramsite when using municipal sludge to burn a light-weight and high-strength ceramsite.

CONCLUSION

In this paper, solid waste such as municipal sludge and coal gasifier slag were used as raw materials to obtain ceramsite with excellent performance through orthogonal experiments. The reasons that affect the performance of the ceramsite were studied by MIP pore structure analysis, SEM, and other microscopic testing methods. The results were as follows:

- The burned ceramsite with 5 - 20 % municipal sludge content meets the requirements of the light-weight, high-strength ceramsite according to standard GB/T 17431.2-2010 "Lightweight Aggregate and Its Experimental Method". The compressive strength of sample A1 with 5 % and 20 % municipal sludge content reached 10.3 MPa, and 6.7 MPa, respectively.
- The weight loss of the mixtures in the heating process increased when increasing the municipal sludge content. The municipal sludge increased the porosity and the average pore diameter of the ceramsite. Therefore, the water absorption rate of the ceramsite increased, and the apparent density decreased when the municipal sludge content increased;
- The compressive strength of the ceramsite decreased with an increasing municipal sludge content when the content of SiO_2 and Al_2O_3 remained unchanged. The compressive strength of the ceramsite in group C1 with a sludge content of 20 % decreased by 3.6 MPa compared with that of group A1 with 5 % content;
- The change in Al_2O_3 content was also the reason for the change in the ceramsite strength when the municipal sludge content was maintained at a constant rate. The main crystal phase of the ceramsite changed from quartz to kyanite when the Al_2O_3 content increased (generally exceeded 20 %), which significantly improves the strength of the ceramsite. Compared with sample A2, the compressive strength of sample A1 with an Al_2O_3 increase of 4.54 % increased by 4.5 MPa.

Acknowledgments

The authors want to acknowledge the financial support of the China West Construction Group Co., Ltd., science and technology research and development foundation (ZJXJ-2019-14). The authors would like to thank all the reviewers who participated in the review and MJEditor (www.mjeditor.com) for its linguistic assistance during the preparation of this manuscript.

REFERENCES

1. Hagemann S E., Gastaldini A L G., Cocco M., Jahn, S. L., Terra, L. M. (2019): Synergic effects of the substitution of Portland cement for water treatment plant sludge ash and ground limestone: technical and economic evaluation. *Journal of Cleaner Production, 214*, 916–926. doi: 10.1016/j.jclepro.2018.12.324
2. Cremades L V., Cusidó J A., Arteaga F. (2018): Recycling of sludge from drinking water treatment as ceramic material for the manufacture of tiles. *Journal of Cleaner Production, 201*, 1071–1080. doi: 10.1016/j.jclepro.2018.08.094
3. Ahmad T., Ahmad K., Alam M. (2017): Sludge quantification at water treatment plant and its management scenario. *Environmental. Monitoring and Assessment, 189*(9), 1–10. doi: 10.1007/s10661-017-6166-1
4. Kocbek E., Garcia H A., Hooijmans C M., Mijatovi I., Brdjanovic D. (2020): Microwave treatment of municipal sewage sludge: evaluation of the drying performance and energy demand of a pilot-scale microwave drying system. *Science of The Total Environment*, *742*, 140541. doi: 10.1016/j.scitotenv.2020.140541
5. Ooi T Y., Yong E L., Din M F M., et al. (2018): Optimization of aluminium recovery from water treatment sludge using response surface methodology. *Journal of Environmental Management, 228*, 13–19. doi: 10.1016/j.jenvman.2018.09.008
6. Ahmad T., Ahmad K., Alam M. (2016): Sustainable management of water treatment sludge through 3'R' concept: Journal of Cleaner Production, 124: 1-13.doi:10.1016/j.jclepro. 2016.02.073
7. Qian J S., Xie C B., Xie X L., et al. (2014): Utilization of Municipal Sewage Sludge as Building Materials: A State of the Art Review. *Journal of Building Materials, 17*(5), 829-836. doi: 10.3969/j.issn.1007-9629.2014.05.013

8. Samuel D C G., Zhou J L., Li W., et al. (2019): Progress in manufacture and properties of construction materials incorporating water treatment sludge: A review. *Resources Conservation & Recycling, 145*, 148-159. doi: 10.1016/j.resconrec.2019.02.032
9. Xu Z H., Liu J G., Song M Y., Zhang Z F.(2013): Effect of temperature on sintering ceramisite with sewage sludge and sediment. *Chinese Journal of Environmental Engineering, 7*(05), 1894-1900.
10. Ding Q J., Wang C., Huang X L. (2014) Study on expansion of sludge spherical ceramsite prepared by sludge and shale. *New Building Materials, 41*(11), 1-4.
11. Liu M W., Wang C Z., Bai Y., Xu G R. (2018): Effects of sintering temperature on the characteristics of lightweight aggregate made from sewage sludge and river sediment. *Journal of Alloys and Compounds, 748*, 522-527. doi: 10.1016/j.jallcom.2018.03.216
12. Qin J., Cui C., Cui X Y., et al. (2015): Preparation and characterization of ceramsite from lime mud and coal fly ash. *Construction and Building Materials, 95*, 10-17. doi: 10.1016/j.conbuildmat.2015.07.106
13. Liu Y Y., Xia T., Wang S X. (2016): Study on Ceramsite Production with Sludge and Sea Mud in Municipal Sewage Plant. *Industrial Safety and Environmental Protection, 42*(3),18 -21. doi: 10.3969/j.issn.1001-425X.2016.03.006
14. Su Z Y., Yu J., Wang C Liu J Q., Hu J. (2014): Preparation of lightweight and high specific surface area ceramsites with sewage sludge. *Journal of Shenzhen University (Science and Technology Edition), 31*(4),374-378. doi: 10.3724/SP.J.1249.2014.04374
15. Qin J Y, Feng S, Fang J, Zhang M H., Jiao Y J., Chen X X. (2019): Effect of silica on structural strength and porosity of sintered ceramsite of sludge. *New Building Materials, 46*(09), 117-122.
16. Zou J L., Xu G R., Li G B. (2009): Ceramsite obtained from water and wastewater sludge and its characteristics affected by Fe_2O_3, CaO, and MgO. *Journal of Hazardous Materials, 165*(1-3), 995-1001. doi: 10.1016/j.jhazmat.2008.10.113
17. Xu G R., Zou J L., Li G B. (2009): Ceramsite obtained from water and wastewater sludge and its characteristics affected by $(Fe_2O_3+CaO+MgO)/(SiO_2+Al_2O_3)$. *Water Research, 43*(11), 2885-2893. doi: 10.1016/j.watres.2009.03.046
18. Zhao H L., Liu F., Liu H Q., Wang L., Hao Y. (2020): Comparative life cycle assessment of two ceramsite production technologies for reusing municipal solid waste incinerator fly ash in China. *Waste Management, 113*, 447-455. doi: 10.1016/j.wasman.2020.06.016
19. Tsai C., Wang K., Chiou I. (2006): Effect of SiO_2-Al_2O_3-flux ratio change on the bloating characteristics of lightweight aggregate material produced from recycled sewage sludge. *Journal of Hazardous Materials, 134*(1-3), 87-93. doi: 10.1016/j.jhazmat.2005.10.035
20. Tong D Y., Liu C M., Liu Y L., Ma C. (2019): Research Status of Ceramsite Prepared from Solid Waste in China. *Protection and Utilization of Minerals, 039*(003), 140-150. doi: 10.13779/j.cnki.issn1001-0076.2019.03.022
21. Qin J., Cui C., Cui X Y., Hussain A.(2015) Preparation and characterization of ceramsite from lime mud and coal fly ash. *Construction and Building Materials, 95*, 10-17. doi: 10.1016/j.conbuildmat.2015.07.106
22. Luo L Q., Tu X., Zhou P F. (2018): Preparation and application of sludge ceramsite prepared from sludge. *China Mining, 27*(11), 151-157.
23. Qu J S., Zhang J B., Sun Z G., Sun Z G., Yang C N., Shi D., Li S P., Li H Q. (2020): Research progress on comprehensive utilization of coal gasification slag. 026(001), 184-193. doi: 10.13226/j.issn.1006-6772.20010301
24. Yang S,. Shi L. J. (2013): Component analysis of coal gasification fine slag and discussion on comprehensive utilization. *Coal Chemical Industry, 41*(4), 29-31. doi: 10.3969/j.issn.1005-9598.2013.04.009
25. Riley C M. (2006): Relation of chemical properties to the bloating of clay. *Journal of the American Ceramic Society, 34*(4), 121-128. doi: 10.1111/j.1151-2916.1951.tb11619.x
26. Yang Y. H., Wei Z. A., Chen Y. L., Li Y. J., Li X. Y. (2017): Utilizing phosphate mine tailings to produce ceramisite: *Construction and Building Materials, 155*, 1081-1090. doi: 10.1016/j.conbuildmat.2017.08.070
27. GB/T 17431.2-2010 (2010). Lightweight Aggregates and its Test Methods-Part 2: Test Methods for Lightweight Aggregates (in Chinese).
28. GB/T 17431.1-2010 (2010). Lightweight aggregates and its test methods. http://cx.spsp.gov.cn/
29. Li X., He C., Lv Y., Shou W J,. Dong B J. (2020): Utilization of municipal sewage sludge and waste glass powder in production of lightweight aggregates. *Construction and Building Materials, 256*, 119413. doi: 10.1016/j.conbuildmat.2020.119413
30. Xu G., Zou J., Li G. (2008): Ceramsite made with water and wastewater sludge and its characteristics affected by SiO_2 and Al_2O_3. *Environmental Science & Technology, 42*(19), 7417. doi: 10.1021/es801446h
31. Kumar R., Bhattchajee B. (2003): Porosity, pore size distribution and in situ strength of concrete. *Cement and Concrete Research, 33*, 155–164. doi: 10.1016/S0008-8846(02)00942-0
32. Das B B., Kongraivednhan B. (2012): Implication of pore size distribution parameters on compressive strength, permeability and hydraulic diffusivity of concrete. *Construction and Building Materials, 28*(1), 382–386. doi: 10.1016/j.conbuildmat.2011.08.055
33. Ma H., Xu B., Liu J., et al. (2014) Effects of water content, magnesia-to-phosphate molar ratio and age on pore structure, strength and permeability of magnesium potassium phosphate cement paste. *Materials and Design, 64*(64), 497–502. doi: 10.1016/j.matdes.2014.07.073
34. Li C., Lee W. J., Huang K. L,. Sheng F. F., Yi C. E. (2007): Vitrification of chromium electroplating sludge. *Environmental Science & Technology, 41*, 2950–2956. doi: 10.1021/es062803d